A Mössbauer spectroscopy and neutron diffraction study of magnetostrictive, melt-spun Fe-Ga alloy ribbons

N J Mellors[a], X Zhao[b], L M Simmons[a], C J Quinn[a] and S H Kilcoyne[c]

[a] Materials and Physics Research Centre, College of Science and Technology, University of Salford, Salford, M5 4WT, UK

[b] Manchester Materials Science Centre, University of Manchester, Manchester, M13 9PL, UK

[c] School of Applied Sciences, University of Huddersfield, Huddersfield, HD1 3DH, UK

Corresponding author: Professor S H Kilcoyne, School of Applied Sciences, University of Huddersfield, Queensgate, Huddersfield, HD1 3DH, UK. Telephone: +44(0)1484 472499, email: s.h.kilcoyne@hud.ac.uk

Abstract

Ribbons of $Fe_{100-x}Ga_x$ (x = 15, 17.5, 19.5 and 22.5) were prepared by rapid solidification from the melt. ^{57}Fe Mössbauer spectroscopy and high resolution neutron diffraction have revealed that $Fe_{100-x}Ga_x$ alloys with x = 15 and 17.5 have the disordered bcc (A2) structure even after annealing, but the alloy with x = 19.5 developed the short-range ordered $D0_3$ phase when annealed. The x = 22.5 alloys showed mainly $D0_3$ phase with a fraction of bcc phase. A fraction of the bcc phase transformed into $D0_3$ phase and the long-range ordering of $D0_3$ phase was improved after annealing. ^{57}Fe Mössbauer spectra showed no observable $L1_2$ phase in any samples even though less than 1% volume of $L1_2$ phases have been found in the annealed samples by neutron diffraction. The additional absorption at hyperfine field of 25 T in x = 22.5 samples was regarded as a result of imperfect $D0_3$ structure, rather than a $L1_2$ phase.

Keywords: Melt spun FeGa alloys; Magnetostrictive alloys; Mössbauer spectroscopy; neutron diffraction; Short-range order; Ferromagnetism

Highlights:

- Melt-spun $Fe_{100-x}Ga_x$ alloys with $(15 \leq x \leq 17.5)$ have a disordered bcc structure.
- Ribbons with x = 19.5 develop short-range ordered $D0_3$ phase upon annealing.
- The x = 22.5 ribbons show mainly $D0_3$ phase with a fraction of bcc phase.

1. Introduction

The iron-gallium alloy system $Fe_{100-x}Ga_x$, has attracted a great deal of attention over the last few years as promising magnetostrictive material for sensor or actuator applications. The alloys exhibit superior magnetostrictive properties at low field, negligible magnetic hysteresis, high mechanical strength, good ductility, and low cost [1-3]. Although the exact nature of this magnetostrictive behaviour is still to be understood, recent studies have suggested that there is a close correlation between the structure of these alloys and their resulting magnetostrictive performance [4-6]. Therefore in order to understand the origin of the magnetostrictive effect in Fe-Ga alloys, knowledge of both the phase constitutions and the short range ordering within these phases is required.

According to widely accepted literature, equilibrium and metastable phase diagrams suggest three possible phases in the $Fe_{100-x}Ga_x$ ($15 < x \leq 30$) alloys. In the equilibrium phase diagram of bulk FeGa alloys, a disordered body-centred cubic (bcc) α-Fe (A2) phase, an ordered bcc ($D0_3$) phase and an ordered face-centred cubic (fcc) phase ($L1_2$) can exist [7], whilst the metastable phase diagram of single crystal samples indicates the possibility of the disordered A2 phase with Ga distributed at random, a B2 simple cubic structure with Fe or Ga occupying the centre position of the bcc structure randomly and the $D0_3$ phase where the Ga occupies alternate centre positions [8]. Rapid cooling of Fe_{100-x} Ga_x crystals (with $18 < x < 21$) results in an alloy entirely in the A2 phase [9]. However, the phase formation after slow cooling is open to debate: Lograsso *et al* established that bulk $Fe_{100-x}Ga_x$ alloys with $18 < x < 21$ and cooled at a rate of 2 °C/min exhibited a two-phase mixture of A2 and $D0_3$ [5], a similar result was noted by Zhang *et al* in $Fe_{81}Ga_{19}$ ribbons cooled at 1.29 °C/min [10]. However, in the same paper [10] a cooling rate in the range 0.43 to 0.26 °C/min was reported to result in the precipitation of an fcc phase into the A2 matrix. Such a result has also been noted by Zhao *et al* in $Fe_{80.5}Ga_{19.5}$ ribbons slow cooled from 1000 °C [11].

Early work on FeGa crystals suggested that the local short-range ordering of the Ga atoms along <100> directions in rapidly quenched $Fe_{100-x}Ga_x$ bcc alloys near $x = 19$ is responsible for the increase

in magnetostriction and that the formation of the ordered $D0_3$ phase in annealed alloys or in those with higher Ga content results in a decrease in magnetostriction [1, 12 and references therein]. However, an alternative suggestion was put forward by Khachaturyan that magnetostriction in melt spun ribbons is a result of the reorientation of $D0_3$ precipitates in the bcc A2 matrix when an external field is applied [13].

Experimental confirmation of these hypotheses still remains a challenge [5, 14] particularly as the phase diagram and the magnetostrictive behaviour of the alloys is strongly dependent upon the form of the alloy (bulk, single crystal, thin film, melt spun ribbon etc). It is difficult to confirm the $D0_3$ ordering in Fe–Ga alloys using standard diffraction techniques because, with the exception of the satellite peaks corresponding to the ordered superlattice structure, many of the peaks corresponding to both $D0_3$ and *A2* phases overlap. In addition, the similarity in the atomic scattering factors of Fe and Ga in this system results in extremely weak superlattice reflections making identification almost impossible using *x*-ray diffraction. High resolution neutron diffraction might be expected to give more informative results since the difference between the neutron scattering factors of Fe and Ga atoms is more pronounced and almost constant with the change of scanning angles [15]. The value of this technique in structural analysis has been proven to be significant [11]. Mössbauer spectroscopy, in contrast, is sensitive to short-range order, and is capable of distinguishing between ordered and disordered atomic structures. There is much experimental literature dating from the early 1970s reporting the use of ^{57}Fe Mössbauer spectroscopy for the investigation of Fe-Ga alloys [16-18]. However, in more recent studies of Fe-Ga alloys the benefit of using Mössbauer spectroscopy in the investigation of Ga-Ga pairing in the $D0_3$ phase of $Fe_{100-x}Ga_x$ alloys has been highlighted [19].

The formation of Ga-Ga clusters in FeGa alloys and the effect of these clusters on the alloys' magnetostrictive properties has been the subject of much debate. The presence of Ga clusters was proposed by Hall in 1957 as a possible explanation of the existence of strain in highly magnetostrictive FeGa alloys in the disordered A2 phase [20]. In 2004, Lui *et al* [21] suggested that the magnetostriction in $Fe_{85}Ga_{15}$ ribbons was a result of the formation of Ga clusters within the

ribbons, while Dunlap *et al* [19] suggested that rapidly quenched samples of $Fe_{91.7}Ga_{8.3}$ showed a small amount of Ga-Ga pairing which increased significantly as the Ga concentration increase to ~20 at %. However, more recently Pascarelli *et al* [22] have stated that their EXAFS and XANES studies show that Ga clustering does not occur in their melt spun $Fe_{80}Ga_{20}$ alloys. Instead they propose an approximately random substitution of Ga on Fe sites which introduces local strain, and hence the magnetostrictive behaviour observed in their ribbons. They also have evidence of strain inducing local defects in the form of second shell Ga-Ga pairs, and claim that their work supports the total energy calculations of Cullen *et al* [23] that show that the large magnetostriction seen in these alloys is due to this strain. Clearly more work needs to be carried out in this area to resolve this dichotomy.

In the present work the extent to which the disordered bcc phase can be retained at room temperature by melt spinning and how this phase contributes to an increase of magnetostriction is explored using a combination of neutron diffraction and Mössbauer spectroscopy.

2. Experimental methods

Ingots of $Fe_{100-x}Ga_x$ with x = 15, 17.5, 19.5, 22.5 were prepared by co-melting the appropriate amounts of high purity (> 99.9%) constituent elements in an argon arc furnace. The ingots were turned and re-melted multiple times to ensure homogeneity. Ribbon samples were produced by melting 3 grams of ingot with an induction coil in a partial argon atmosphere and ejecting the melt onto the surface of a rapidly rotating copper wheel. The peripheral speed of the wheel was approximately 35 ms^{-1}. The orifice diameter of the quartz crucible was approximately 0.5 mm. The resulting polycrystalline ribbons were typically 30 μm thick, 5 mm wide and of lengths varying between 10-100 mm. A fraction of the ribbons were sealed in a quartz tube under approximately one atmosphere of argon, heated at 1000°C for one hour and then cooled slowly to room temperature.

Neutron diffraction experiments were carried out on both as-quenched and annealed ribbons on the D2B diffractometer, at the ILL Grenoble, France [24]. Approximately 2g of ribbons were packed into vanadium cans and diffraction patterns were collected from 0 to 158° at ambient temperature by using

the high-resolution mode with a scanning step size of 0.05°. Room-temperature ^{57}Fe Mössbauer effect spectra were collected in transmission geometry using a Rh^{57}Co source and a Wissel System Mössbauer spectrometer operating in the sinusoidal mode, with the γ-ray perpendicular to the ribbon plane. All spectra were referenced to a room-temperature α-Fe pattern. The intrinsic spectrometer line width is approximately 0.10 mm s^{-1} (FWHM). Details of the fitting procedures used for spectral analysis are described in section 3.2.

3. Results

3.1 Neutron Diffraction

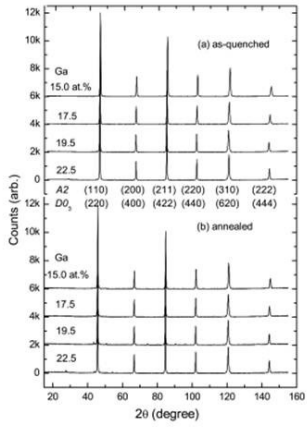

Figure 1

The neutron diffraction patterns from both as-quenched and annealed ribbons are shown in figure 1. The six strong diffraction peaks can be easily identified as arising from the bcc A2 structure or the corresponding reflections from the $D0_3$ structure. Diffraction patterns from the ribbons with x = 19.5 and 22.5 are emphasized in figure 2, in which the portion between $2\theta = 20^o$ to 110^o has been enlarged and shows the existence of small additional peaks in the pattern. One group belongs to the vanadium can used in the experiment. Vanadium is bcc with a = 3.0297 Å, and gives rise to diffraction peaks on the left of the *A*2 peaks. One such peak is clearly seen at $2\theta \sim 41^o$ in all the patterns.

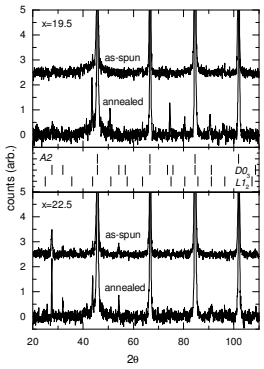

Figure 2.

Additional reflections were observed in the patterns from both the annealed and the as quenched ribbons, and are particularly obvious in the x =19.5 pattern. These new peaks have been indexed and are associated with a Fe_3Ga $L1_2$ phase. This was unexpected, as it is generally believed that the $L1_2$ phase is very difficult to form and we have not observed this phase in annealed FeGa bulk samples with a similar composition (unpublished results). It is clear that a significant volume of the $D0_3$ phase has not formed in the x = 19.5 ribbon as no obvious Bragg peaks from $D0_3$ can be seen even in the low intensity part of the diffraction pattern. This suggests a structural transformation from $A2$ to $L1_2$, rather than from $D0_3$ to $L1_2$ during the annealing process. When the Ga content is increased to 22.5 at %, extra reflections arising from the ordered Fe_3Ga $D0_3$ structure are observed. There is some agreement between these results and those of Zhang *et al* [25,26]. In their work melt spun ribbons of $Fe_{100-x}Ga_x$ with x = 17 and 19 exhibit the distorted bcc (A2) structure. This phase remains in the x = 19 sample after annealing but is accompanied by the $D0_3$ phase when the x = 17 sample is annealed, a result which is not seen in this work.

The lattice parameters for all eight samples were determined using the diffraction fitting software package GSAS [27]. There is good agreement between these lattice parameters and those determined by Dunlap *et al* [19], where ribbons of $Fe_{100-x}Ga_x$ with x = 8.3, 17.9, 20.5 and 23.3 were also shown to

form in the A2 structure when quenched. The results of this work together with the results of Dunlap *et al* [19] and Luo [28] are shown in figure 3, where it can be seen that in all three systems the lattice parameter increases approximately linearly as the Ga concentration increases at a rate of 1.9 x 10^{-4} nm / at %.

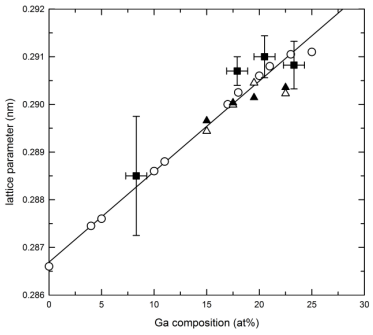

Figure 3.

A more detailed discussion of the neutron diffraction data is given in an earlier paper by Zhao *et al* [11], but to summarise: The high-resolution neutron diffraction spectra shown in figures 1 and 2 indicate that only diffraction peaks arising from the disordered bcc *A2* phase are present in as-quenched x = 15, 17.5 and 19.5 ribbons, without any trace of satellite or split peaks. Post annealing $L1_2$ reflections appeared, and are most prominent in the x = 19.5 alloy. In contrast, the as-quenched x = 22.5 ribbons contain traces of both the A2 and $D0_3$ phase, furthermore, upon annealing it is noted that that fractions of the A_2 phase are transformed into the $D0_3$ phase.

3.2 Mössbauer Spectroscopy

Room-temperature ^{57}Fe Mössbauer spectra of both as-quenched and annealed ribbons are shown in figure 4. It is apparent that all samples are ferromagnetically ordered at room temperature as six line spectra are observed for all compositions. However there are some variations in the form of the magnetic order. The spectra from ribbons with x = 15, and 17.5 exhibit only broadened sextets while

the spectra from x = 19.5 samples start to show additional, sharper features. The x = 22.5 spectra are noticeably

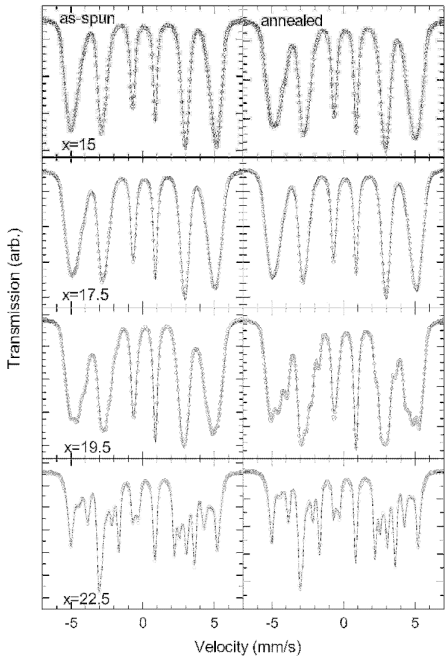

Figure 4

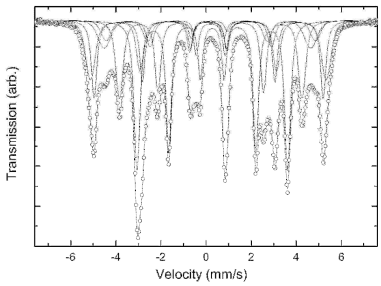

Figure 5.

different to those alloys with lower Ga content, showing several resolvable sextets that suggest some structural changes and a much greater degree of local ordering as the Ga content has increased. Rancourt *et al* [29,30] have shown that it is appropriate to model Mössbauer spectra from such materials as a combination of Gaussian-distributed Lorentzian sextets. Each sextet was described using an isomer shift δ, a mean hyperfine field value <H>, a width, σ_H, and an area A. The quadrupole shift was assumed to be zero in all cases. The relative areas of the six spectral peaks were constrained to be 3:y:1:1:y:3 where y was determined during the fit.

The spectra from both the annealed and the quenched ribbons with x = 15 and 17.5 were best fitted using two sextets, and the resulting hyperfine field distributions are illustrated in figure 6. The mean values of the hyperfine fields decrease with the increase of Ga content. Annealing has little effect on the hyperfine field in these samples, except to reduce the hyperfine fields of the x = 15 sample slightly. The spectra from the x = 19.5 ribbons show more features than observed in the spectra from ribbons with x = 15 and 17.5. In order to model these additional features four sextets are needed to fit the as-quenched spectrum, while the spectrum from the annealed x = 19.5 ribbon is best fitted with six sites. The parameters for the best fits for spectra from ribbons with x = 15, 17.5 and 19.5 are shown in Table 1. For $x \leq 20$ the variation in mean hyperfine field value is approximately linear with Ga composition decreasing at a rate of 0.18 T /at %.

There have been several Mössbauer studies on FeGa alloys. For example Conversion Electron Mössbauer Spectroscopy (CEMS) was used to study thin film samples of $Fe_{100-x}Ga_x$ with $10 \leq x \leq 35$ [31,32]. Blachowski *et al* [33] have carried out a Mössbauer study of $Fe_{100-x}Ga_x$ ingots with $10 \leq x \leq 29$. However as the structural examinations have shown, the phase-composition diagrams vary for different forms of the alloys and therefore it is only really useful to compare the results of this study with the results obtained from studies of rapidly quenched material. Newkirk and Tsuei [16] examined quenched $Fe_{100-x}Ga_x$ foils ~35μm thick . For $0 \leq x \leq 20$ the samples gave broad six line Mössbauer spectra, while the sample with x = 25 gave a spectrum with sharper lines arising from several distinct magnetic sites. Similarly Dunlap *et al*'s study of melt spun $Fe_{100-x}Ga_x$ ribbons showed broad six line Mössbauer spectra from samples with $8.3 \leq x \leq 20$, which were best fitted with a distribution of hyperfine fields. When x was increased to 23.5 the spectrum became much sharper, showing three clearly resolved sextets. In both these studies the spectra were comparable to those obtained in this work from the as-quenched samples (displayed on the left hand side of figure 4). Neither Newkirk and Tsuei nor Dunlap *et al* examined annealed alloys.

These results of the fits to the Mössbauer spectra from ribbons with $15 \leq x \leq 19.5$ are shown in figure 7, where the agreement of this work with the results of Newkirk and Tsuei [16] and Dunlap *et al* [19] can be observed.

Visual inspection of the resolvable absorption peaks in the spectrum of as-spun $x = 22.5$ ribbon suggests the presence of at least four distinct sites, however, in practice six distinct sites are needed to obtain a good fit to this spectrum. The final fit is shown in figure 5, with the resulting hyperfine field distribution in figure 6. The mean hyperfine parameters for the six sites are summarized in Table 2. The values of y (not shown) from the fit to this spectrum, are greater than 2, suggesting the existence of a small amount of in-plane magnetic texture. It should be noted that this is in complete contrast to the results of Dunlap *et al* [19] where the spectra from as-quenched samples with $8.3 \leq x \leq 23.3$ could be fitted with $1.95 \leq y \leq 2.09$, indicating that there is no evidence for magnetic texture in their samples.

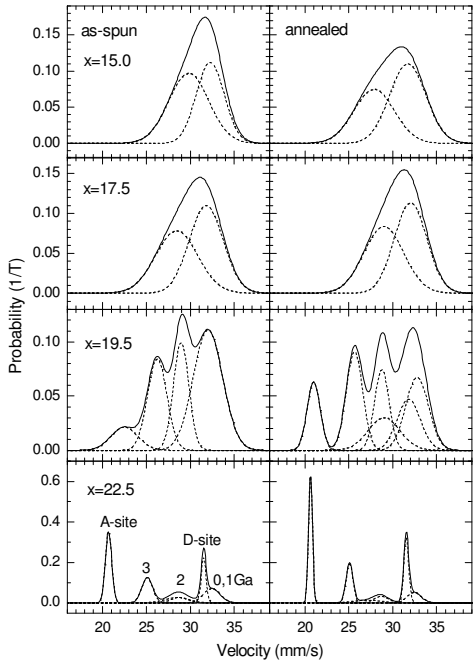

Figure 6.

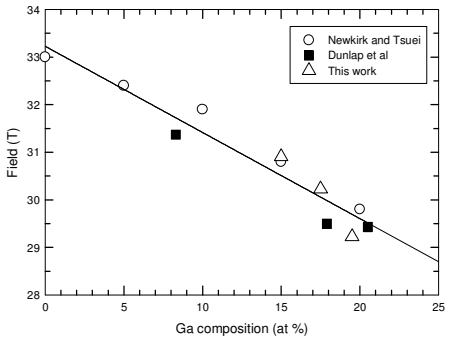

Figure 7.

x = 15 as-spun					*x* = 15 annealed				
Site	<H> (T)	σ_H (T)	δ (mm s^{-1})	*A* (%)	Site	<H> (T)	σ_H (T)	δ (mm s^{-1})	*A* (%)
1	32.26	1.59	0.04	44.6	1	31.71	2.07	0.09	56.96
2	29.83	2.28	0.13	55.4	2	27.87	2.30	0.16	43.04

x = 17.5 as-spun					x = 17.5 annealed				
1	31.80	1.94	0.07	53.2	1	32.03	1.85	0.07	52.5
2	28.45	2.39	0.16	46.8	2	28.99	2.27	0.15	47.5
x = 19.5 as-spun					x = 19.5 annealed				
1	31.80	1.94	0.07	53.2	1	32.03	1.85	0.07	52.5
2	28.45	2.39	0.16	46.8	2	28.99	2.27	0.15	47.5
3	31.80	1.94	0.07	53.2	3	32.03	1.85	0.07	52.5
4	28.45	2.39	0.16	46.8	4	28.99	2.27	0.15	47.5
					5	32.03	1.85	0.07	52.5
					6	28.99	2.27	0.15	47.5

Table 1. ^{57}Fe Mössbauer effect parameters for the sites obtained from the fits to the spectra from the ribbons with x = 15, 17.5 and 19.5 as described in the text. The velocity scale is referenced to the α-Fe spectrum at room-temperature.

x = 22.5 as-spun						x = 22.5 annealed					
Site	<H> (T)	σ_H (T)	δ (mm s^{-1})	A (%)	Description	Site	<H> (T)	σ_H (T)	δ (mm s^{-1})	A (%)	Description
1	32.42	0.94	0.10	16.9	< 6 Ga NNN	1	32.43	0.79	0.09	10.4	< 6 Ga NNN
2	31.51	0.27	0.11	15.4	$D0_3$ D-site	2	31.55	0.28	0.11	22.5	$D0_3$ D-site
3	28.78	1.00	0.21	7	2 Ga NN	3	28.66	0.85	0.15	7.03	2 Ga NN
4	28.42	1.36	0.06	9.2	2 Ga NN	4	27.14	1.59	0.00	5.3	2 Ga NN
5	25.10	0.62	0.21	19.3	3 Ga NN	5	25.09	0.38	0.21	18.6	3 Ga NN
6	20.70	0.36	0.28	32.1	$D0_3$ A-site	6	20.65	0.23	0.28	36.1	$D0_3$ A-site

Table 2. ^{57}Fe Mössbauer effect parameters for the sites obtained from the fits to the spectra of ribbons with x = 22.5 as described in the text. The velocity scale is referenced to the α-Fe spectrum at room-temperature.

4. Discussion

For a random distribution of Ga on the bcc Fe lattice, assuming a binomial distribution and that the eight nearest neighbours have the nominal composition, we expect the probability, P(n), of Fe sites with n Ga nearest neighbour to be

$$P(n) = \frac{8!}{n!(8-n)!}\left(\frac{x}{100}\right)^{n}\left(1-\frac{x}{100}\right)^{8-n} \quad (1)$$

For the x = 15 and 17.5 samples, the probability of Fe sites with 0 or 1 Ga nearest neighbours is calculated as 0.66 and 0.58 respectively. However, it is found that the relative area of the sites at higher field is 45% and 53% respectively which is less than the calculated value. This seems to indicate the distribution of Ga in the bcc phase is not entirely random and that Ga prefers sites with a high number of Ga nearest neighbours. Initially this phenomenon was regarded as evidence of the enhancement of Ga-Ga pairing [19]. However, the assumption above completely neglects the fact that the central atom must be an Fe atom. When taking the central Fe atom and the eight nearest neighbours as a whole and assuming its Ga content is x, the Ga content in the nearest neighbours should be 9x/8, instead of x. With this new Ga content and equation 1, the probability of sites with 0 or 1 Ga atom is 0.60 and 0.51 for x = 15 and 17.5 ribbons respectively, which is closer to the observed value.

At least four sextets were needed to fit the spectrum from the as-quenched x = 19.5 ribbon, corresponding to the sites with 0 or 1 Ga nearest neighbour, 2, 3, and 4 Ga nearest neighbours respectively. The resulting hyperfine field distributions are shown in figure 6. The mean hyperfine

fields and isomer shifts change approximately linearly with the number of Ga neighbours. The probabilities calculated from Equation 1 are 0.52, 0.29, 0.14 and 0.04 for the four sites mentioned above. The relative areas of sites at 32.0, 29.0, 26.2 and 22.5 T are 46.7, 21.9, 23.3 and 8.2 % respectively. Again this seems to indicate that the distribution of Ga in the *A2* phase in these ribbons is not entirely random but that Ga prefers Ga nearest neighbours. However, the calculated probability of the site with two Ga nearest neighbours is higher than the observed 21.9%, suggesting no improvement in the Ga-Ga pairing although the disordered bcc Fe-Ga alloys of this composition demonstrate the highest magnetostriction. In contrast, the relative area of the site with four Ga nearest neighbours is double that predicted, indicating the formation of high Ga content clusters or even the short-range ordered $D0_3$ precipitates in the bcc A2 matrix. It is possible these $D0_3$ precipitates might be responsible for the increase in magnetostriction of high Ga content Fe-Ga alloys, as predicted in [14].

The absorptions in the Mössbauer spectrum from the annealed ribbon with $x = 19.5$ occur at the hyperfine fields similar to those observed in the $x = 22.5$ spectrum. All three spectra were best fitted using six sextets. In the $x = 19.5$ ribbon the absorption at around 21 T is well separated from other peaks, and is believed to be attributed to Fe sites with four Ga nearest neighbours, similar to the A-sites of $D0_3$, indicating the formation of $D0_3$ phase after annealing treatment. However, the broader distribution of this site suggests the formed $D0_3$ phase is probably only short-range ordered. This is confirmed by its neutron diffraction pattern where no obvious superlattice diffractions from $D0_3$ phase can be found. The relative area of this site fitted from the spectrum is 12%, which corresponds to a $D0_3$ volume of approximately 18% in this sample when assuming the number of A-sites is twice that of D-sites.

In the spectrum from the as-quenched $x = 22.5$ ribbon the two sites with hyperfine fields of 20.7 and 31.5 T and narrow field distributions correspond well to the values of the $D0_3$ phase reported by others [17,19], with room-temperature Fe hyperfine field values of 20.5 and 31.2 T for the $D0_3$ phase and 26.9 T for the $L1_2$ phase in Fe_3Ga samples [17], and 20.69 and 31.44 T for the $D0_3$ phase and

25.30 T for the $L1_2$ phase in x=23.3 samples [19]. The two fields for the $D0_3$ structure correspond to the so-called A-sites with four Fe and four Ga nearest neighbours and six Fe next nearest neighbours (NNN), and D-sites with eight Fe nearest neighbours and six Ga next nearest neighbours. We believe that the reasonable agreement of the hyperfine fields for those samples, suggests a conventional Ga–Ga pairing along <110> directions which occurs in the $D0_3$ structure. However, the site with a hyperfine field of 25.08T is expected to be a Fe site similar to A-sites of $D0_3$ but with only three Ga and five Fe nearest neighbours, rather than $L1_2$ site as suggested previously [19]. It is reported that the Fe_3Ga $L1_2$ phase has one hyperfine field at 26.9 T with two quadrupole shifts [16]. In the present work, there is no need to introduce quadrupole shifts to obtain a better fit suggesting no observable $L1_2$ absorptions in the samples. However, despite the fact that neutron diffraction patterns show no $L1_2$ phase in the as-quenched ribbons, they do reveal a trace of $L1_2$ phases in the annealed samples, most notably in the x = 19.5 ribbons although the volume of such a phase is estimated to be less than 1% , which is not discernable in the Mössbauer spectra. In contrast, the relative area of absorption with a hyperfine field of 25.08 T is around 19 %.

The two sites with a hyperfine field of around 28.6 T are considered as Fe sites with two Ga and six Fe nearest neighbours, the difference in the isomer shift value might indicate a difference in the Ga pair arrangement, either along the <100>, <110> or <111> directions. The site with a hyperfine field of 32.45 T has an isomer shift value identical to that of $D0_3$ D-sites, suggesting this site is similar to D-sites but with fewer Ga atoms as its next nearest neighbours. As the absorption area is much higher than the site with two Ga nearest neighbours, it is very likely the absorption with a hyperfine field of 32.45 T has a contribution from the site having one Ga nearest neighbour, as the sites with 0 or 1 Ga nearest neighbours in disordered bcc phase are believed to have similar hyperfine fields [16]. The occurrence of sites with hyperfine fields around 28.6 T and 32.45 T indicates the existence of disordered bcc Fe-Ga phase in this sample.

Comparing the hyperfine field distributions of the x=22.5 ribbons pre- and post annealing treatment (lower section of figure 6), one can see that the hyperfine field distributions of A-sites and D-sites of

annealed samples become narrower, suggesting an improvement of chemical ordering in the $D0_3$ phase, and that the corresponding probabilities are also higher than those of as-quenched ribbons while the probabilities of bcc sites mentioned above become lower. The probability increases from 32.1% to 36.1% for A-sites, and 15.4% to 22.5% for D-sites. This is consistent with neutron diffraction results where the integrated intensities of $D0_3$ superlattice peaks at $2\theta \sim 27.5^{o}$ and 57.2^{o}, normalized to the (220) peak, increases from 2.14% and 0.82% to 2.40% and 1.07% respectively after annealing, with an uncertainty of ±0.05%. The increases in both the peak intensities of neutron diffraction and the relative areas of Mössbauer spectrum indicate an increase in the volume of $D0_3$ phase after annealing, which in turn confirms that there may be an *A2* phase in the as-quenched ribbons and a transformation from an A2 phase into $D0_3$ phase after annealing.

5. Conclusions

^{57}Fe Mössbauer spectroscopy and neutron diffraction have been used to study as quenched and annealed samples of melt spun $Fe_{100-x}Ga_x$ alloys. Neutron diffraction has shown that ribbons with x = 15 and 17.5 have the disordered bcc (A2) structure both before and after annealing, but ribbons with x = 19.5, which has the A2 structure initially, develops short-range ordered $D0_3$ phase upon annealing. The ribbons with x = 22.5 show mainly $D0_3$ phase with a fraction of bcc phase, moreover, some of the bcc phase transforms into $D0_3$ phase and the long-range ordering of $D0_3$ phase was improved after annealing.

Room temperature Mossbauer spectroscopy has shown that all samples are ferromagnetically ordered. At low Ga concentrations there is a distribution of hyperfine fields in the samples, centered around ~29T and ~32T for both the as spun and annealed ribbons. However, as the Ga concentration is increased beyond ~19 at % there is a much greater degree of local order in the material with four distinct Fe sites in the x = 19.5 as quenched ribbons and six distinct Fe sites in the x = 19.5 annealed ribbons and in both the x = 22.5 as quenched and annealed ribbons.

These results also demonstrate the suitability of ^{57}Fe Mössbauer spectroscopy for studying the formation of $D0_3$ ordering that cannot be observed by conventional diffraction techniques due to either insufficiently long range ordering or, as in the Fe–Ga system, because of the closeness of the elements' atomic scattering factors. Mössbauer spectroscopy together with neutron diffraction can build a detailed knowledge of the structural properties of these alloys and help to correlate this structural information to changes in the magnetostriction and help understand the causes underlying the formation of a large magnetostriction.

Acknowledgements

This work was generated in the context of the MESEMA project, funded under the 6th Framework Programme of the European Community _Contract No. AST3-CT-2003-502915. Dr N. Lupu and Professor H. Chiriac from the National Institute of Research and Development for Technical Physics, Romania are gratefully acknowledged for their help with the sample preparation.

Figure captions

Figure 1. Room temperature neutron diffraction patterns of as-quenched and annealed $Fe_{100-x}Ga_x$ ribbons with x = 15, 17.5, 19.5, 22.5).

Figure 2. Expanded room temperature neutron diffraction pattern of as-quenched and annealed x = 19.5 and x = 22.5 $Fe_{100-x}Ga_x$ alloy ribbons. Tick marks for the A2, $D0_3$ and $L1_2$ phases are shown in the central panel.

Figure 3. Room temperature lattice parameter of the bcc phase as a function of Ga content. The values are taken from Luo (○) [23], Dunlap *et al* (■) [19] and this work (▲△).

Figure 4. Room-temperature ^{57}Fe Mössbauer spectra of $Fe_{100-x}Ga_x$ ribbons. Circles represent experimental data, the solid lines going through circles are the best fit.

Figure 5. Room-temperature ^{57}Fe Mössbauer spectra of as-spun x = 22.5 ribbons. Circles represent experimental data, the solid lines going through circles are the best fit. The individual sub-spectra are shown as thin solid lines.

Figure 6. Room-temperature Fe hyperfine field distributions in $Fe_{100-x}Ga_x$ ribbons The distributions for the individual spectral components are shown by the broken lines and the total distribution is shown by the solid line.

Figure 7. Mean hyperfine fields calculated from room temperature spectra of quenched samples with x = 15, 17.5 and 19.5. The plot includes results from Newkirk and Tsuei (○) [16], Dunlap *et al* (■) [19] and the present work (△).

References

[1] J.R. Cullen, A.E. Clarke, M. Wun-Fogle, J.B. Restorff and T.A.Lograsso, Journal of Magnetism and Magnetic Materials 226-230 (2001) 948-949

[2] R.A. Kellogg, A.B. Flatau, A.E. Clark, M. Wun-Fogle and T.A. Lograsso, Journal of Applied Physics 91 (2002) 7821-7823

[3] A.E. Clark, M. Wun-Fogle, J.B. Restorff and T.A. Lograsso, Materials Transactions 43 (2002) 881-886.

[4] A.E. Clark, K.B. Hatherway, M. Wun-Fogle, J.B. Restorff, T.A. Lograsso, V.M. Keppens and G. Perculescu, Journal of Applied Physics 91 (2003) 8621-8623

[5] T.A. Lograsso and E.M. Summers Materials Science and Engineering 416 (2006) 240-245

[6] J. Zhang, T. Ma and M Yan, Physica B 404 (2009) 4155-4158

[7] O. Ikeda, R. Kainuma, I. Ohnuma, K. Fukamichi and K. Ishida, Journal of Alloys and Compounds 347 (2002) 198-205

[8] Y. Du, M. Huang, S. Chang, D.L. Schlagel, T.A. Lograsso and R.J. McQueeney, Physical Review B 81 (2010) 054432 1-9

[9] H. Cao, F.M. Bai, J.F. Li, D.D. Viehland, T.A. Lograsso and P.M. Gehring, Journal of Alloys and Compounds 465 (2008) 244-249

[10] J. Zhang, T. Ma and M. Yan, Journal of Magnetism and Magnetic Materials. 322 (2010) 2882-2887

[11] X. Zhao, N.J. Mellors, S.H. Kilcoyne, D. Lord, N. Lupu, H. Chiriac and P.F. Henry, Journal of Applied Physics 103 (2008) 07B320

[12] C. Li, J. Liu, Z. Wang and C. Jiang, Journal of Magnetism and Magnetic Materials 324 (2012) 1177-1181

[13] A.G. Khachaturyan and D.D. Viehland, Metallurgical and Materials Transactions 38A (2007) 2308-2316

[14] T.A. Lograsso, A.R. Ross, D.L. Schlagel, A.E. Clarke and M. Wun-Fogle, Journal of Alloys and Compounds 350 (2003) 92-101

[15] G.E. Bacon, Neutron Diffraction. 3rd Ed, Clarendon Press, Oxford, UK (1975)

[16] L.R. Newkirk and C.C. TsueI, Physical Review B4 (1971) 4046

[17] N. Kawamiya, K. Adachi and Y. Nakamura, Journal of Physics Society Japan 33 (1972) 1318-1327

[18] G.K. Wertheim, V. Jaccarino, J.H. Wernick and D.N.E. Buchanan, Phyical Review Letters 12 (1964) 24-27

[19] R.A. Dunlap, J.D. McGraw and S.P. Farrell, Journal of Magnetism and Magnetic Materials 305 (2006) 315-320

[20] R.C. Hall, Journal of Applied Physics 28, (1957) 707

[21] G.D. Lui, L.B. Liu, Z.H. Liu, M. Zhang, J.L. Chen, J.Q. Li, G.H. Wu, Y.X. Li, J.P. Qu and T.S. Chin, Applied Physics Letters 84, (2004) 2124-2126

[22] S. Pascarelli, M.P. Ruffoni, R. Sato Turtelli, F. Kubel and R. Grössinger, Physical Review B77, (2008) 184406

[23] J. Cullen, P. Zhao and M. Wuttig, Journal of Applied Physics 101 (2007) 123922

[24] D2B High resolution two axis diffractometer www.ill.eu/instruments-support/instruments-groups/instruments/d2b/

[25] M. C. Zhang, H. L. Jiang, X. X. Gao, J. Zhu, and S. Z. Zhou Journal of Applied Physics, 99, (2006) 023903

[26] J. Zhang, T. Ma, M. Yan, Physica B 404, (2009) 4155

[27] A.C. Larson and R.B. Von Dreele, General Structure Analysis System (GSAS), Los Alamos National Laboratory Report LAUR (1994) 86-748

[28] H.L. Luo, Trans Metall Soc AIME 239 (1967) 119

[29] D.G. Rancourt and J.Y. Ping, Nuclear Instruments and Methods in Physics Research section B58 (1991) 85-97

[30] K. Lagarec and D.G. Rancourt, Nuclear Instruments and Methods in Physics Research section B129 (1997) 266-280

[31] A. Javed, N.A. Morley, T. Szumiata and M.R.J. Gibbs, Applied Surface Science 257, (2011) 5977-5983

[32] T. Szumiata, K Brzozka, M. Gawronski, B. Gorka, A Javed, N.A. Morley and M.R.J. Gibbs. Acta Physica Polonica A 119, (2011) 21

[33] A. Blachowski, K. Ruebenbauer, J. Zukrowski and J. Przewoznik, Journal of Alloys and Compounds 455, (2008) 47